

# Axion Mie theory for a spherical topological insulator

Johannes Schultz<sup>1\*</sup>, Flavio S. Nogueira<sup>2</sup>, Bernd Büchner<sup>1,3</sup>, Jeroen van den Brink<sup>2,4</sup>, Axel Lubk<sup>1,3</sup>

**1** IFW Dresden, Helmholtzstraße 20, 01069 Dresden, Germany

**2** Institute for Theoretical Solid State Physics, IFW Dresden, Helmholtzstraße 20, 01069 Dresden, Germany

**3** Department of Physics, TU Dresden, 01069 Dresden, Germany

**4** Institute for Theoretical Physics, TU Dresden, 01069 Dresden, Germany

\*j.schultz@ifw-dresden.de

June 8, 2022

## Abstract

Electronic topological states of matter exhibit novel types of responses to electromagnetic fields. The response of strong topological insulators, for instance, is characterized by a so-called axion term in the electromagnetic Lagrangian which is ultimately due to the presence of topological surface states. Here we develop the axion Mie theory describing the electromagnetic response of spherical particles including an axion electromagnetic coupling at the surface of a particle. The approach includes arbitrary sources of fields, i.e., charge and current distributions. We derive an axion induced mixing of transverse magnetic and transverse electric modes which are experimentally detectable through small induced rotations of the field vectors.

---

## Contents

<b>1</b>	<b>Introduction</b>	<b>2</b>
<b>2</b>	<b>Solution of the field equations</b>	<b>4</b>
<b>3</b>	<b>Conclusion</b>	<b>12</b>
<b>A</b>	<b>Helmholtz Decomposition of Dielectric Response</b>	<b>13</b>
<b>B</b>	<b>Mie Theory</b>	<b>13</b>
	B.1 Field equations in spherical coordinates	13
	B.2 Boundary Conditions	16
	<b>References</b>	<b>19</b>

---

## 1 Introduction

It has been long known theoretically that in CP-violating theories topological defects become electrically charged, one of the most prominent examples being the induced fractional electric charge in 't Hooft-Polyakov monopoles [1]. This result follows immediately from the presence of a CP-violating interaction in the Lagrangian of the gauge theory,

$$\mathcal{L}_a = \frac{\Theta g^2}{64\pi^2} \epsilon_{\mu\nu\lambda\rho} F^{\mu\nu} F^{\lambda\rho}, \quad (1)$$

where  $F_{\mu\nu}$  is the usual field strength tensor of the gauge sector of the theory and  $g$  is the gauge coupling. The significance of the parameter  $\Theta$  varies depending on the context, but we will refer to it here simply as the *axion*, in reference to the chiral (or axial) anomaly [2]. Within an Abelian gauge theory context, observable consequences of axion electrodynamics have been discussed for some time, with references to materials already being made in early papers. For instance, Nielsen and Ninomiya [3] mentioned HgCdTe and Wilczek [4] discusses an application of axion electrodynamics to PbTe, following a suggestion by Fradkin *et al.* [5]. However, it was not until more recently with the prediction and discovery of several topological materials, notably topological insulators (TIs) [6,7] and Weyl semimetals [8], that the many possible interesting experimental consequences of axion electrodynamics came closer to spotlight. In this work we mainly focus on TIs, but the theory described here applies with minor modifications to Weyl semimetals as well.

Three-dimensional TIs feature a quantum Hall electromagnetic response at the surface, which emerges as a consequence of an insulator behavior in the bulk characterized effectively by the following axion electrodynamics Lagrangian [9],

$$\mathcal{L} = \frac{1}{8\pi} (\epsilon \mathbf{E}^2 - \mathbf{B}^2) - \frac{\alpha\Theta}{4\pi^2} \mathbf{E} \cdot \mathbf{B}, \quad (2)$$

where  $\mathbf{E}$  and  $\mathbf{B}$  are the electric and magnetic field, respectively,  $\alpha = e^2/(\hbar c)$  is the fine-structure constant and we have assumed a paramagnetic bulk with magnetic permeability  $\mu = 1$ . For TIs where either time-reversal or inversion symmetry holds,  $\Theta = \pi$ . Thus, a TI sample in vacuum may be considered as the problem of a topological dielectric satisfying the Maxwell equations,

$$\nabla \cdot \left( \epsilon \mathbf{E} - \frac{\alpha\Theta}{\pi} \mathbf{B} \right) = 4\pi\rho, \quad (3)$$

$$\nabla \times \left( \mathbf{B} + \frac{\alpha\Theta}{\pi} \mathbf{E} \right) = ik \left( \epsilon \mathbf{E} - \frac{\alpha\Theta}{\pi} \mathbf{B} \right) + \frac{4\pi}{c} \mathbf{j}, \quad (4)$$

$$\nabla \times \mathbf{E} + ik\mathbf{B} = 0, \quad (5)$$

$$\nabla \cdot \mathbf{B} = 0, \quad (6)$$

where we have used  $\mathbf{E} \rightarrow \mathbf{E}e^{-ickt}$ ,  $\mathbf{B} \rightarrow \mathbf{B}e^{-ickt}$ , current  $\mathbf{j} \rightarrow \mathbf{j}e^{-ickt}$ , charge density  $\rho \rightarrow \rho e^{-ickt}$ , and assumed a frequency-dependent dielectric function,  $\epsilon(\omega, \mathbf{r}) = \epsilon(ck, \mathbf{r})$ . Using eq. (5), we can rewrite eq. (4) as,

$$\nabla \times \mathbf{B} + i\epsilon k \mathbf{E} = \frac{4\pi}{c} \mathbf{j} - \frac{\alpha}{\pi} \nabla \Theta \times \mathbf{E}. \quad (7)$$

Note that since  $\Theta$  is uniform inside the TI and vanishes outside it,  $\nabla\Theta$  is proportional to a delta function on the TI surface,  $\Sigma_{TI}$ . From the above equation we can easily read off the surface quantum Hall current,

$$\mathbf{j}_H(\mathbf{r}) = \frac{e^2\Theta}{2\pi h} \int d\mathbf{S}(u, v) \times \mathbf{E}(\mathbf{r}) \delta^3(\mathbf{r} - \mathbf{r}_S(u, v)), \quad (8)$$

where  $d\mathbf{S}(u, v) = dudv[\partial\mathbf{r}_S(u, v)/\partial u \times \partial\mathbf{r}_S(u, v)/\partial v]$  and  $\mathbf{r}_S(u, v) \in \Sigma_{TI}$ , with  $(u, v) \in \mathbb{R}^2$  being associated to a parametrization of  $\Sigma_{TI}$ . We have that  $\sigma_H = e^2\Theta/(2\pi h)$  is the Hall conductivity. For  $\Theta = \pi$  or, more generally,  $\Theta = 2\pi(n + 1/2)$ ,  $n \in \mathbb{Z}$ , we obtain a half-quantized Hall conductivity [9].

In the past several years a number of predictions of electromagnetic phenomena related to TIs have been made based on the above equations of axion electrodynamics [9–16]. Experimentally, such phenomena are often difficult to probe, since some effects manifest themselves only through corrections  $\sim \mathcal{O}(\alpha^2)$ . There are effects occurring at  $\mathcal{O}(\alpha)$ , which are more accessible to experimental probes. This is precisely the case with, for instance, the Faraday and Kerr rotation in TIs [9, 11], which has been measured using  $\text{Bi}_2\text{Se}_3$  [17] and strained HgTe [18] samples. The derivation of the effect is elementary and follows directly from the Maxwell equations above with the boundary conditions modified by the discontinuity of  $\Theta$  across the TI surface [9].

Another  $\mathcal{O}(\alpha)$  effect that has been predicted in the literature concerns surface plasmon polaritons (SPPs) on the planar surface of a TI [12]. In this work the standard analysis of SPPs on a planar geometry has been extended to TIs in the same geometry. As a matter of fact, the same Maxwell equations can be used, except for a nontrivial change in the boundary conditions due to the presence of the axion term in eq. (2) [12]. Indeed, the TI surface introduces a discontinuity in  $\Theta$  mixing electric and magnetic boundary conditions even in the static case [10, 14, 16]. As a consequence, while there is only a transverse magnetic (TM) and no transverse electric (TE) component of the electric field in the usual theory for SPPs on planar surfaces, such a component does not vanish in the TI case.

One of the most important effects of light scattering beyond the planar geometry originates from the so called Mie theory [19]. This theory deals with plane wave scattering by a dielectric sphere and amounts to solving the Maxwell equations with appropriate boundary conditions [20, 21]. Developing the *axion Mie* theory is severely complicated by the disparity between the spherical symmetry of the target relative to the incoming plane waves; including the axion modifies the boundary conditions relative to the standard Mie theory calculations. Even if certain aspects of the Mie theory for spherical TIs has been considered recently [22], there are many relevant issues that remain to be resolved. This includes an accurate treatment of the modified boundary conditions beyond the first order perturbation level as well as the incorporation of arbitrary sources of fields (i.e., charges and currents) and the identification of suitable experimental setups allowing to measure the implications of the axion term. Another important distinction between the standard Mie theory for a dielectric sphere and the corresponding extension to the spherical TI case is that the latter has a metallic surface where induced (surface) currents feature electrons with the spin-momentum locking property. The latter is actually responsible for the peculiar electromagnetic response whose content is captured by the Lagrangian (eq. (2)).

In the following we elaborate on these general considerations restricting ourselves to spherical symmetry. This allows to derive analytical solutions for the electromagnetic response of TI

spheres, notably including Hall currents, magnetic fluxes, and scattering cross-sections. Our considerations essentially amount to an extension of classical Mie theory to include the ramification of the axion term. Herein we do not restrict ourselves to the charge- and current-free case typically subsumed under Mie theory and allow for arbitrary external sources of fields. We will, however, focus somewhat on particular case of localized surface plasmons (LSPs), i.e., negative dielectric response bands. This serves as an archetypal model system for the LSPs on TI nanoparticles of more complicated shape, noting that in particular topological characteristics do not depend on the particular particle shape. For other regimes of positive dielectric response, which may be treated with the same formalism, we refer to the literature.

## 2 Solution of the field equations

In order to describe the dielectric response of a TI the curl of the Maxwell eq. (4) is computed inserting eq. (5) to replace the magnetic flux density

$$\nabla \times (\nabla \times \mathbf{E}) - k^2 \epsilon \mathbf{E} + ik \frac{\alpha}{\pi} \nabla \Theta \times \mathbf{E} = i \frac{4\pi k}{c} \mathbf{j}. \quad (9)$$

For later use we also note an alternative form of the equation valid for spatially constant  $\epsilon$

$$-\Delta \mathbf{E} - k^2 \epsilon \mathbf{E} + ik \frac{\alpha}{\pi} \nabla \Theta \times \mathbf{E} = i \frac{4\pi k}{c} \mathbf{j} - \frac{4\pi}{\epsilon} \nabla \rho. \quad (10)$$

The general dielectric response of the sphere (i.e. Mie theory) is obtained by solving the response eq. (9) exploiting spherical symmetry. In the following we tackle the problem by a piecewise solution in regions of spatially constant  $\epsilon$  and  $\Theta$  (i.e., within and outside of the sphere) and fixing the missing integration constants through appropriate boundary conditions. Apart from assuming spherical symmetry, there are no approximations in the expressions above and in this spirit we will continue below when presenting the exact solution of the problem. It is furthermore informative to perform a Helmholtz decomposition of the dielectric response equation at this state as it allows to distinguish a longitudinal and transverse part of the solution on this very fundamental level (see Appendix A). We will make use of these results further below.

We begin with expanding the electric field into vector spherical harmonics (following the definition of Barrera et al. [23])

$$\mathbf{E}(\mathbf{r}) = \sum_{l=0}^{\infty} \sum_{m=-l}^l \left( E_{lm}^{\perp}(r) \mathbf{Y}_{lm} + E_{lm}^{(1)}(r) \mathbf{\Psi}_{lm} + E_{lm}^{(2)}(r) \mathbf{\Phi}_{lm} \right), \quad (11)$$

which form a complete basis for vector fields in three dimensions and hence give rise to a general representation of electric and magnetic fields adapted to spherical coordinates. That notably also includes fields beyond free vacuum solutions, which are typically considered in the literature of Mie scattering. Such free solutions may be represented by a restricted set of only two vector spherical harmonics as discussed further below [20]. Note furthermore that the  $l=0$  case is peculiar in that both  $\mathbf{\Psi}$  and  $\mathbf{\Phi}$  vanish identically (ultimately a consequence of the hairy ball theorem). As a consequence the  $l=0$  modes play a special role throughout.

Taking into account the completeness relations of the vector spherical harmonics eqs., (9) and (10) reduce to a system of three ordinary differential equations for each vector spherical harmonics (see Appendix B). After setting  $E_{lm}^{\perp} = E_{lm}^{(\perp)}/r$  we explicitly obtain

$$\begin{aligned}
& r^2 \frac{d^2 E_{lm}^{(\perp)}}{dr^2} + 2r \frac{dE_{lm}^{(\perp)}}{dr} + (k^2 \epsilon r^2 - l(l+1)) E_{lm}^{(\perp)} \\
&= -i \frac{4\pi k}{c} r j_{lm}^\perp + \frac{12\pi}{\epsilon} r (\nabla \rho)_{lm}^{(1)} + \frac{4\pi}{\epsilon} r^2 \frac{d(\nabla \rho)_{lm}^{(1)}}{dr}
\end{aligned} \tag{12}$$

for the first component  $E^{(\perp)}$ . The second component  $E^{(1)}$  is directly linked to the first through the first Maxwell equation

$$E_{lm}^{(1)} = \frac{r}{l(l+1)} \frac{dE_{lm}^\perp}{dr} + \frac{2}{l(l+1)} E_{lm}^\perp - \frac{4\pi}{\epsilon l(l+1)} r^2 (\nabla \rho)_{lm}^{(1)}. \tag{13}$$

Note that the apparent divergence in case of  $l = 0$  dissolves under closer inspection as the  $\Psi$  component vanishes. The third differential equation for  $E^{(2)}$  has again the same mathematical structure as the first

$$r^2 \frac{d^2 E_{lm}^{(2)}}{dr^2} + 2r \frac{dE_{lm}^{(2)}}{dr} + (r^2 k^2 \epsilon - l(l+1)) E_{lm}^{(2)} = -i \frac{4\pi k}{c} j_{lm}^{(2)}. \tag{14}$$

Both, the first and third, are inhomogeneous second order differential equation in  $E_{lm}^{(\perp)}$  of (modified) spherical Bessel type (after absorbing  $k\sqrt{\epsilon} = kn$  into  $r$ ). The fate of the equation being of modified type or not is decided by the sign of the index of refraction  $n = \sqrt{\epsilon}$ . While in vacuum  $n$  is positive corresponding to a spherical Bessel equation, within the sphere both positive and negative sign (depending on the frequency) can occur. In the following, we consider the negative sign leading to evanescent excitations (i.e., surface plasmons) confined to the surface of the sphere. Note, however, that the general solution (notably including whispering gallery modes when  $\epsilon_{\text{sphere}} > \epsilon_{\text{vac}}$ ) for general complex-valued  $\epsilon$  follow straightforwardly utilizing Bessel functions of complex arguments. Note furthermore that the solution space can be further restricted to those, which do not diverge at the origin.

The general solutions of the above differential equations split into a homogeneous and inhomogeneous part. The homogeneous solution, which includes the important problem of light scattering on a sphere (i.e. Mie scattering), is considered first. Subsequently, we will also discuss the general inhomogeneous case. General solutions without external sources (the homogeneous solutions) for the above second order differential equation may be generally expanded into two fundamental solutions, which are spherical Bessel functions in our case. For the radial component (eq. (12)) this expansion explicitly reads

$$E_{lm}^{(\perp)}(r) = \begin{cases} a_l^{(\perp)} i_l(nkr), & r < R \\ b_l^{(\perp)} j_l(kr) + c_l^{(\perp)} y_l(kr), & r \geq R. \end{cases} \tag{15}$$

Note that the modified Bessel function of second kind does not appear in the interior of the sphere as it diverges at the origin. From eq. (13) the first tangential component can be derived

$$E_{lm}^{(1)}(r) = \begin{cases} a_l^{(\perp)} \left[ \frac{nk}{l(l+1)} i_{l+1}(nkr) + \frac{1}{l} \frac{i_l(nkr)}{r} \right], & r < R \\ b_l^{(\perp)} \frac{r k j_{l-1}(kr) + l j_l(kr)}{r l(l+1)} + c_l^{(\perp)} \frac{r k y_{l-1}(kr) + l y_l(kr)}{r l(l+1)}, & r \geq R. \end{cases} \tag{16}$$

The solution to eq. (14) for the second tangential component reads

$$E_{lm}^{(2)}(r) = \begin{cases} a_l^{(2)} i_l(nkr), & r < R \\ b_l^{(2)} j_l(kr) + c_l^{(2)} y_l(kr), & r \geq R. \end{cases} \quad (17)$$

In the first case the magnetic field is strictly tangential to the sphere, whereas in the second case the electric field is tangential. Moreover, the first set of solutions is curl-free (longitudinal), whereas the the second one is divergence-free (transverse) in the electrical field. While the latter are called transverse electric (TE), the first go under the name longitudinal electric, quasi-static or transverse magnetic (TM) depending on the context. Both modes are completely decoupled (and orthogonal) in the topologically trivial case. Note furthermore that in both cases the homogeneous solutions are degenerate with respect to  $m$ .

In order to determine the six expansion coefficients (remember that  $E^{(1)}$  can be computed once  $E^{(\perp)}$  is known) of the homogeneous solutions above a corresponding number of boundary conditions has to be provided. Four of them stem from the internal boundaries at the surface of the sphere. The remaining two are given by normalization conditions. Indeed, it is only at this stage, where deviations from the classical Mie theory are introduced by the axion term, as anticipated. The internal boundary conditions are derived from partial derivatives normal to the surface inserting Maxwell's equations as usual.

From the homogeneous Maxwell equations (second and third) we obtain

$$\frac{r dE_{lm1}^{\perp}}{dr} + 2E_{lm1}^{\perp} = \frac{r dE_{lm2}^{\perp}}{dr} + 2E_{lm2}^{\perp} \quad (18)$$

and

$$-\frac{l(l+1)}{r} \left( E_{lm1}^{(2)} - E_{lm2}^{(2)} \right) = 0. \quad (19)$$

The BCs obtained from the inhomogeneous Maxwell equations (first and fourth) read

$$E_{lm2}^{\perp} - n^2 E_{lm1}^{\perp} = \frac{i\alpha}{k\pi} \frac{l(l+1)}{r} E_{lm}^{(2)} \Theta \quad (20)$$

and

$$-\frac{ik\alpha}{\pi l(l+1)} \left( r \frac{dE_{lm}^{\perp}}{dr} + 2E_{lm}^{\perp} \right) \Theta = \frac{dE_{lm1}^{(2)}}{dr} - \frac{dE_{lm2}^{(2)}}{dr}. \quad (21)$$

Similarly to the field equations only 2 of the 4 BCs are affected by the topological term (i.e., those pertaining to the inhomogeneous Maxwell equations), while the other two remain as in the classical Mie theory.

We finally solve the system of BCs for the 6 coefficients  $a_l$ ,  $b_l$ ,  $c_l$ . The solutions for  $b_l^{(2)}$ ,  $c_l^{(2)}$ ,  $b_l^{(\perp)}$  and  $c_l^{(\perp)}$  in terms of  $a_l^{(\perp)}$  and  $a_l^{(2)}$  read

$$b_l^{(2)} = \frac{a_l^{(2)} \left( y_l \frac{di_l}{dr} - i_l \frac{dy_l}{dr} \right)}{y_l \frac{dj_l}{dr} - j_l \frac{dy_l}{dr}} + \frac{a_l^{(\perp)} \frac{ik\alpha\Theta}{\pi l(l+1)} \frac{d(ri_l)}{rdr} y_l}{y_l \frac{dj_l}{dr} - j_l \frac{dy_l}{dr}} \quad (22)$$

$$c_l^{(2)} = \frac{a_l^{(2)} \left( j_l \frac{di_l}{dr} - i_l \frac{dj_l}{dr} \right)}{j_l \frac{dy_l}{dr} - y_l \frac{dj_l}{dr}} + \frac{a_l^{(\perp)} \frac{ik\alpha\Theta}{\pi l(l+1)} \frac{d(ri_l)}{rdr} j_l}{j_l \frac{dy_l}{dr} - y_l \frac{dj_l}{dr}} \quad (23)$$

$$b_l^{(\perp)} = \frac{a_l^{(\perp)} \left( y_l \frac{d(ri_l)}{rdr} - n^2 i_l \frac{d(ry_l)}{rdr} \right)}{y_l \frac{dj_l}{dr} - j_l \frac{dy_l}{dr}} + \frac{a_l^{(2)} \frac{\alpha l(l+1)\Theta}{ik\pi} \frac{d(ry_l)}{rdr} i_l}{y_l \frac{dj_l}{dr} - j_l \frac{dy_l}{dr}} \quad (24)$$

$$c_l^{(\perp)} = \frac{a_l^{(\perp)} \left( j_l \frac{d(ri_l)}{rdr} - n^2 i_l \frac{d(rj_l)}{rdr} \right)}{j_l \frac{dy_l}{dr} - y_l \frac{dj_l}{dr}} + \frac{a_l^{(2)} \frac{\alpha l(l+1)\Theta}{ik\pi} \frac{d(rj_l)}{rdr} i_l}{j_l \frac{dy_l}{dr} - y_l \frac{dj_l}{dr}} \quad (25)$$

From the equations above it is clear that indeed the modifications due to the axion term amount to a mixing of the originally decoupled TM and TE solutions, which has been previously noted for the half-plane boundary case by Karch [12]. Noting that TM and TE fields are perpendicular, their weak mixing is equivalent to a rotation of the electric or magnetic field vectors linear in  $\alpha$ , which has been successfully detected in the half plane geometry and may be also amenable to experimental detection in case of the sphere.

Fixing  $a_l^{(\perp)}$  and  $a_l^{(2)}$  by orthonormalizing the corresponding fields lead to the so-called normal modes. This procedure amounts to a separate normalization of the TM and TE modes in the topologically trivial case. In case of the non-trivial case we avoid the tedious orthonormalization in the following and fix the coefficients  $a_l^{(\perp)}$  and  $a_l^{(2)}$  through simpler approximations (motivated by the smallness of the topological term). Fig. 1 shows a comparison between classical TM and TE normal modes for  $l = 1$  and the corresponding TI solutions (normalized by setting  $a_l^{(\perp)}$  or  $a_l^{(2)}$  to zero, respectively). In the topologically trivial setting (left columns of Fig. 1 respectively) we readily observe that TM and TE normal modes are completely decoupled. In case of the TI sphere on the right columns of Fig. 1 respectively, on the other hand, originally purely TM and TE modes mix due to the axion term, i.e., acquire a small TE and TM character respectively. Similarly, the 3D representation of the  $l = 1, m = 1$  modes (Fig. 2) reveals a tilting out of the tangential plane of the B-field (E-field) in case of the TM (TE) mode, which corresponds to the above noted mixing of TM and TE modes. A notable exception pertains to the  $l = 0$  TM mode, which is magnetic field free and not affected by the modified boundary conditions due to the axion term.

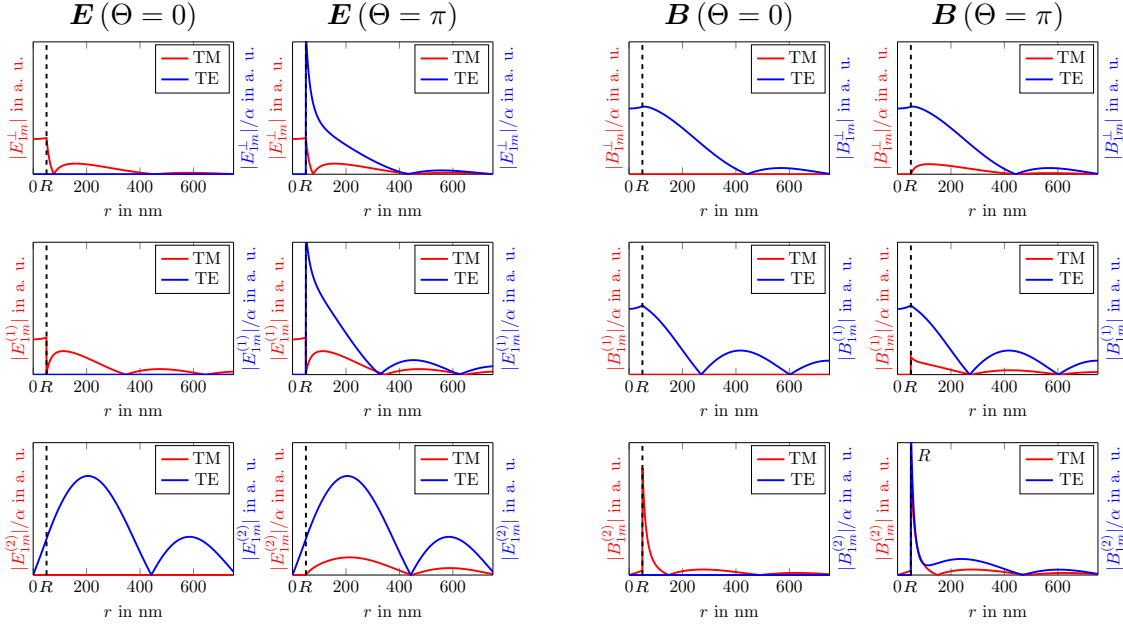


Figure 1: Radial dependency of electric and magnetic field components (absolute value) of  $l = 1$  normal modes for topologically trivial and TI sphere. Note that the y-axis was always scaled in the same arbitrary units.

More insight into the origin of that behaviour may be obtained from the analysis of the Hall currents associated to the axion term (eq. (8) and eq.(21)). Fig. 3 show the Hall current of the  $l = 1, m = 1$  TM mode. Accordingly, the Hall current has a source and sink due to oscillating charges and produces magnetic fields with components normal to the surface, i.e. a TE mode. Moreover, the number of sources and sinks increases with the mode order, e.g., a quadrupolar structure is visible for the  $l = 2, m = 2$  TM mode (see Fig. 3). The above analytic expressions for the normal modes admits an expansion of any electromagnetic response of the TI in the absence to charges and currents, i.e., the description of (resonant) photon scattering. As an example we note the solution to the scattering of a linearly polarized plane wave. Note that due to conservation of angular momentum the whole problem separates in  $l$ . In order to obtain an analytic expression of the scattering and extinction cross section ( $\sigma_s$ , eq. (28) and  $\sigma_e$ , eq. (29)) we first rewrite the normal modes in the vacuum regions in terms of Hankel functions of first and second kind with excitation coefficients  $d_l = \frac{b_l - ic_l}{2}$  and  $e_l = \frac{b_l + ic_l}{2}$  respectively, which allow a separation of incoming and outgoing spherical waves. In a second step the outgoing waves are normalized by the incoming one to obtain the normalized scattered wave and the scattering cross section. Last but not least the coefficients  $a_l^{(\perp)}$  or  $a_l^{(2)}$  are fixed by requiring the outgoing waves  $d_l^{(\perp)}$  or  $d_l^{(2)}$  to be zero respectively. We explicitly



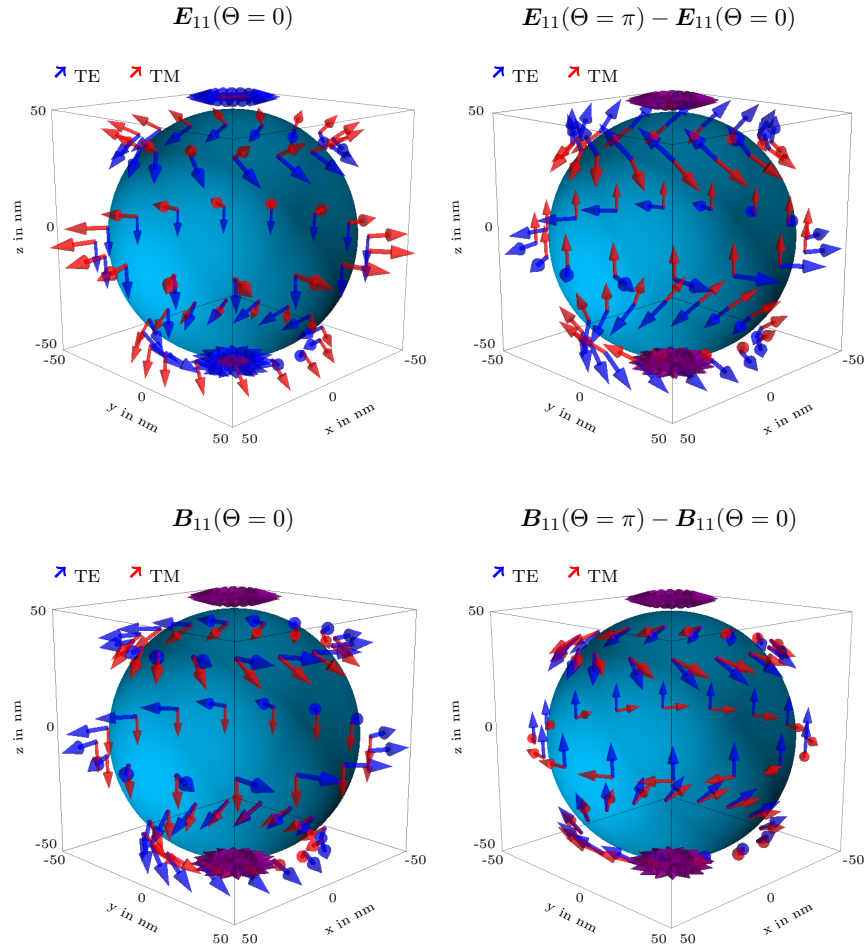


Figure 2: 3D vector representation at  $r = 55$  nm of the  $l = 1, m = 1$  TM and TE modes (absolute value) for the topologically trivial sphere with  $R = 50$  nm (left hand side) and their modifications due to the axion term (right hand side).

obtain for the scattering coefficients  $f_l^{(\perp)}$  and  $g_l^{(\perp)}$

$$f_l^{(\perp)} = -\frac{1}{2} \frac{d_l^{(\perp)} - e_l^{(\perp)}}{e_l^{(\perp)}} = \frac{n^2 i_l \frac{d(rj_l)}{rdr} - j_l \frac{d(ri_l)}{rdr} + \alpha^2 \Theta^2 \zeta \frac{d(rj_l)}{rdr}}{n^2 i_l \frac{d(rh_l^{(1)})}{rdr} - h_l^{(1)} \frac{d(ri_l)}{rdr} + \alpha^2 \Theta^2 \zeta \frac{d(rh_l^{(1)})}{rdr}} \quad (26)$$

$$\text{with } \zeta = \frac{\frac{d(ri_l)}{rdr} h_l^{(2)}}{\pi^2 \left( \frac{di_l}{dr} h_l^{(2)} - i_l \frac{dh_l^{(2)}}{dr} \right)} i_l$$

and

$$g_l^{(2)} = -\frac{1}{2} \frac{d_l^{(2)} - e_l^{(2)}}{e_l^{(2)}} = \frac{i_l \frac{d(rj_l)}{rdr} - j_l \frac{dri_l}{rdr} + \alpha^2 \Theta^2 \xi j_l}{i_l \frac{drh_l^{(1)}}{rdr} - h_l^{(1)} \frac{dri_l}{rdr} + \alpha^2 \Theta^2 \xi h_l^{(1)}} \quad (27)$$

$$\text{with } \xi = \frac{i_l \frac{d(rh_l^{(2)})}{rdr}}{\pi^2 \left( \frac{d(ri_l)}{rdr} h_l^{(2)} - n^2 i_l \frac{d(rh_l^{(2)})}{rdr} \right)} \frac{d(ri_l)}{rdr}$$

respectively. Note that we get an additional factor of  $-\frac{1}{2}$  in the definition of  $f_l^{(\perp)}$  and  $g_l^{(2)}$  in comparison to the well-known classical Mie theory result (see, e.g., [20]). This is a consequence of our choice of the vector spherical harmonics defined by Barrera et al. [23], differing from those used conventionally.

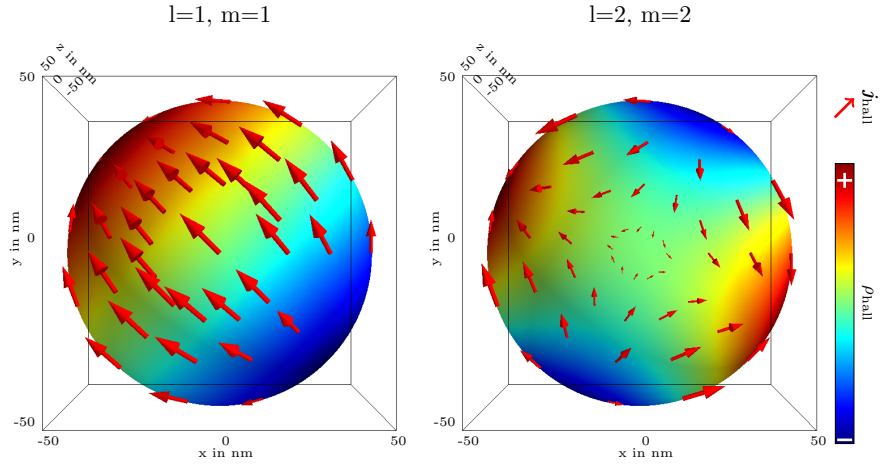


Figure 3: Hall current (real part) of the TM  $l = 1, m = 1/l = 2, m = 2$  mode (vector plot) and the corresponding oscillating charges (color coded). Note that both are coupled by a continuity equation.

The scattering cross section  $\sigma_s$  and extinction cross section  $\sigma_e$  then reads:

$$\sigma_s = \frac{2\pi}{k^2} \sum_{l=0}^{\infty} (2l+1) \left( |f_l^{(\perp)}|^2 + |g_l^{(2)}|^2 \right) \quad (28)$$

and

$$\sigma_e = \frac{2\pi}{k^2} \sum_{l=0}^{\infty} (2l+1) \Re \left\{ f_l^{(\perp)} + g_l^{(2)} \right\} \quad (29)$$

(see eq. (75) and eq. (74) for the full analytic solution). Accordingly, we observe that the well-known classical Mie theory result ( $\Theta = 0$ , see, e.g., [20]) is modified by a topological term of the order  $\alpha^2$  in both the nominator and denominator. While the former slightly shifts the energy of the resonances at zeros of the nominator the latter leads to a modification of the scattering intensity. Due to their smallness both are beyond current experimental detection.

We finally turn our attention to the general inhomogeneous case. As the solution of the pertaining differential eqs. (12) and (14) for arbitrary external currents and charges ultimately requires numerical methods, we restrict our discussion to the highly symmetric case of a broad parallel and fast electron beam, transmitting the TI sphere. That example corresponds to the important experimental setup of electron energy loss spectroscopy in the transmission electron microscope, and allows us to illustrate the general principles and possible novel detection schemes of the axion term.

The electron density and current (in frequency space) of an electron beam moving with velocity  $v$  in  $z$ -direction reads

$$\rho(\mathbf{r}, \omega) = -\frac{\rho_0}{v} e^{i\omega(z-z_0)/v} \quad (30)$$

and

$$\mathbf{j}(\mathbf{r}, \omega) = -j_0 e^{i\omega(z-z_0)/v} \begin{pmatrix} \cos \theta \\ -\sin \theta \\ 0 \end{pmatrix} \quad (31)$$

respectively. Note that the vector components pertain to spherical coordinates, i.e., to coordinate axes pointing into  $r, \theta, \varphi$  directions. For further use we also note the gradient of the charge

$$\nabla \rho(\mathbf{r}, \omega) = -i \frac{\rho_0 \omega}{v^2} e^{i\omega(z-z_0)/v} \begin{pmatrix} \cos \theta \\ -\sin \theta \\ 0 \end{pmatrix}. \quad (32)$$

In the next step we compute the expansion coefficients of the gradient of the charge and the current as appearing in the inhomogeneous differential eqs. (12) and (14). The relevant coefficients for the current read

$$\begin{aligned} j_{lm}^\perp &= -j_0 e^{-i\frac{\omega}{v}z_0} \int e^{i\frac{\omega}{v}r \cos \theta} \cos \theta Y_{l,m}^* d\Omega \\ &= -\sqrt{4\pi(2l+1)} j_0 e^{-i\frac{\omega}{v}z_0} \delta_{m,0} \sum_{\ell'=0}^{\infty} i^{\ell'} j_{\ell'} \left(\frac{\omega}{v}r\right) (2\ell'+1) \begin{pmatrix} l & 1 & \ell' \\ 0 & 0 & 0 \end{pmatrix}^2 \end{aligned} \quad (33)$$

and

$$\begin{aligned} j_{lm}^{(2)} &= \frac{j_0}{l(l+1)} e^{-i\frac{\omega}{v}z_0} \int e^{i\frac{\omega}{v}r \cos \theta} \frac{dY_{l,m}^*}{d\varphi} d\Omega \\ &= i\sqrt{4\pi} \frac{j_0 m}{l(l+1)} (-1)^m e^{-i\frac{\omega}{v}z_0} \sum_{\ell'=0}^{\infty} \sqrt{2\ell'+1} i^{\ell'} j_{\ell'} \left(\frac{\omega}{v}r\right) \int Y_{\ell',0} Y_{l,-m} d\Omega \\ &= 0 \end{aligned} \quad (34)$$

whereas that for the gradient of the charge is

$$\begin{aligned} (\nabla \rho)_{lm}^{(1)} &= i \frac{\rho_0 \omega}{v^2 l(l+1)} e^{-i\frac{\omega}{v}z_0} \int e^{i\frac{\omega}{v}r \cos \theta} \sin \theta \frac{dY_{l,m}^*}{d\theta} d\Omega \\ &= -2\sqrt{2\pi} \rho_0 \sqrt{\frac{2l+1}{l(l+1)}} e^{-i\frac{\omega}{v}z_0} \delta_{m,0} \sum_{\ell'=0}^{\infty} (2\ell'+1) i^{\ell'} j_{\ell'} \left(\frac{\omega}{v}r\right) \begin{pmatrix} l & 1 & \ell' \\ 0 & 0 & 0 \end{pmatrix} \begin{pmatrix} l & 1 & \ell' \\ 1 & -1 & 0 \end{pmatrix} \end{aligned} \quad (35)$$

In case of non-vanishing coefficients we observe that the radial dependency of all inhomogeneous terms is that of a superposition of spherical Bessel functions  $j_\ell$  and the azimuthal dependency is trivial ( $m = 0$ ) as expected for a cylindrical beam. More importantly, we note that the second tangential component of the current vanishes, which means that a broad electron beam cannot excite a TE mode for conventional dielectric spheres. Similar to the homogeneous case, however, that limitation is lifted by the boundary conditions. In that case the coupling of TM and TE components leads to non-vanishing  $E^{(2)}$  components with the excitation strength being linear in  $\alpha$  (see Fig. 4). The precise radial dependency of all coefficients can be obtained by numerically solving eq. (12) and eq. (14) after inserting the above expressions.

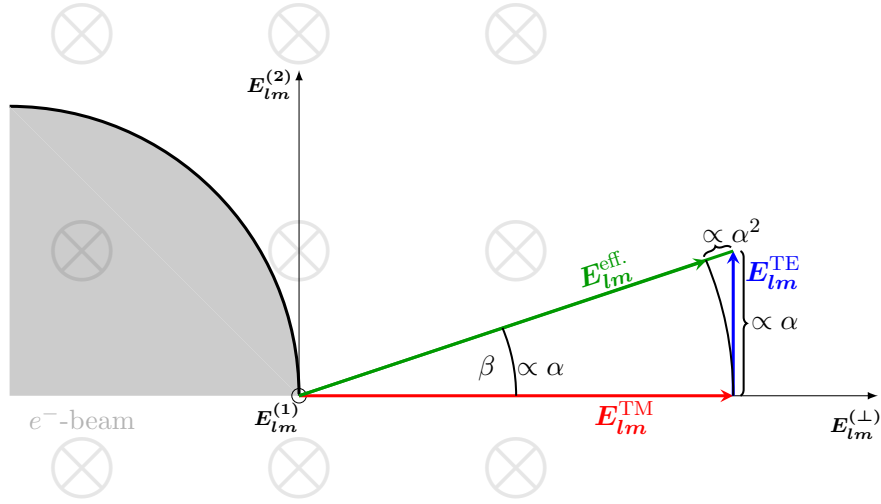


Figure 4: Axion admixing of  $E_{lm}^{TE}$  components to a  $E_{lm}^{TM}$ -mode. The change of the lengths of the resulting effective electric field vector  $E_{lm}^{eff.}$  is of the order  $\alpha^2$  whereas the rotation angle  $\beta$  scales linear with  $\alpha$ .

### 3 Conclusion

In summary, we have extended the description of the electromagnetic response of spherical particles to include the ramifications of an axion term such as present in topological insulators. We have studied the consequences for the excitation of localized surface plasmons on spherical TI nanoparticles. We found an intrinsic mixing of TM and TE modes as leading order effect (linear in  $\alpha$ ). This mixing manifests itself as a small rotation of the induced electric and magnetic fields, which we anticipate to be detectable by suitable setups. Promising candidates utilizing localized probes (i.e. electron beams) are polarization-resolved cathodoluminescence and inelastic momentum transfer measurements [24]. Corresponding shifts in LSP resonance energies and scattering or extinction coefficients, on the other hand, are of the order of  $\alpha^2$ , hence difficult to detect. We also note that the presented formalism allows to include arbitrary external currents and charges, typically not included in the standard formulation of Mie theory. As an example we discussed the dielectric response of a TI sphere transmitted by a broad

electron beam as utilized in electron energy loss spectroscopy.

## Acknowledgments

A.L. received funding from the European Research Council (ERC) under the Horizon 2020 research and innovation program of the European Union (grant agreement no. 715620). J.S. received funding from the Deutsche Forschungsgemeinschaft (DFG, German Research Foundation) under Germanys Excellence Strategy–EXC2147/1 ST0232019 ”Cluster of Excellence on Complexity and Topology in Quantum Matter —ct.qmat”. JvdB acknowledges support from the Deutsche Forschungsgemeinschaft (DFG) through the Collaborative Research Center (Sonderforschungsbereich) SFB 1143 (Project No. 247310070).

## A Helmholtz Decomposition of Dielectric Response

For the classification of the dielectric response of a sphere it is informative to note the Helmholtz decomposition into transverse

$$\begin{aligned} & \nabla \times \nabla \times \mathbf{E}_t - k^2 (\epsilon \mathbf{E})_t + ik \frac{\alpha}{\pi} \nabla \times (\Theta \mathbf{E}) \\ - & ik \frac{\alpha \Theta}{\pi} (\nabla \times \mathbf{E})_t = i \frac{4\pi k}{c} \mathbf{j}_t, \end{aligned} \quad (36)$$

and longitudinal part

$$k^2 (\epsilon \mathbf{E})_l - ik \frac{\alpha \Theta}{\pi} (\nabla \times \mathbf{E})_l = i \frac{4\pi k}{c} \mathbf{j}_l \quad (37)$$

of the fundamental response eq. (9). Note in particular that the first Maxwell equation combined with the continuity equation,

$$i\omega \nabla \cdot \left( \epsilon \mathbf{E} - \frac{\alpha \Theta}{\pi} \mathbf{B} \right) = 4\pi \nabla \cdot \mathbf{j} \quad (38)$$

has the same longitudinal solution

$$i\omega \epsilon \mathbf{E}_l - \frac{\alpha c}{\pi} \Theta \nabla \times \mathbf{E} = 4\pi \mathbf{j}_l. \quad (39)$$

Consequently, the response eq. (9) is sufficient to model plasmonics in frequency domain. The  $\mathbf{B}$ -field is readily obtained after inserting  $\mathbf{E}$  into the third Maxwell equation.

## B Mie Theory

### B.1 Field equations in spherical coordinates

The general dielectric response of the sphere (i.e. Mie theory) is obtained by solving the response eq. (9) exploiting spherical symmetry. In the following we tackle the problem by a piecewise solution in regions of constant  $\epsilon$  and  $\Theta$  (i.e., within and outside of the sphere) and

fixing the missing integration constants through appropriate boundary conditions. Accordingly, the response equation in homogeneous regions reads

$$\nabla \times \nabla \times \mathbf{E} - k^2 \epsilon \mathbf{E} = i \frac{4\pi k}{c} \mathbf{j} \quad (40)$$

or

$$-\Delta \mathbf{E} - k^2 \epsilon \mathbf{E} = i \frac{4\pi k}{c} \mathbf{j} - \frac{4\pi}{\epsilon} \nabla \rho. \quad (41)$$

In the next step we expand the solution into vector spherical harmonics (following the definition of Barrera et al. [23])

$$\mathbf{E}(\mathbf{r}) = \sum_{l=0}^{\infty} \sum_{m=-l}^l \left( E_{lm}^{\perp}(r) \mathbf{Y}_{lm} + E_{lm}^{(1)}(r) \mathbf{\Psi}_{lm} + E_{lm}^{(2)}(r) \mathbf{\Phi}_{lm} \right), \quad (42)$$

which gives us later less headaches, when defining the boundary conditions, compared to the more common Hertz potential expansion. Inserting the expansion into eq. (40) yields

$$\begin{aligned} & \nabla \times \sum_{l=0}^{\infty} \sum_{m=-l}^l \left[ -\frac{l(l+1)}{r} E_{lm}^{(2)} \mathbf{Y}_{lm} - \left( \frac{dE_{lm}^{(2)}}{dr} + \frac{1}{r} E_{lm}^{(2)} \right) \mathbf{\Psi}_{lm} \right. \\ & \left. + \left( -\frac{1}{r} E_{lm}^{\perp} + \frac{dE_{lm}^{(1)}}{dr} + \frac{1}{r} E_{lm}^{(1)} \right) \mathbf{\Phi}_{lm} \right] + k^2 \epsilon \mathbf{E} = i \frac{4\pi k}{c} \mathbf{j} \end{aligned} \quad (43)$$

after evaluating one curl and finally

$$\begin{aligned} & \sum_{l=0}^{\infty} \sum_{m=-l}^l \left[ \left( \frac{l(l+1)}{r^2} E_{lm}^{\perp} - \frac{l(l+1)}{r} \frac{dE_{lm}^{(1)}}{dr} - \frac{l(l+1)}{r^2} E_{lm}^{(1)} - k^2 \epsilon \right) \mathbf{Y}_{lm} \right. \\ & + \left( \frac{1}{r} \frac{dE_{lm}^{\perp}}{dr} - \frac{d^2 E_{lm}^{(1)}}{dr^2} - \frac{2}{r} \frac{dE_{lm}^{(1)}}{dr} - k^2 \epsilon \right) \mathbf{\Psi}_{lm} \\ & \left. + \left( \frac{l(l+1)}{r^2} E_{lm}^{(2)} - \frac{d^2 E_{lm}^{(2)}}{dr^2} - \frac{2}{r} \frac{dE_{lm}^{(2)}}{dr} - k^2 \epsilon \right) \mathbf{\Phi}_{lm} \right] = i \frac{4\pi k}{c} \mathbf{j} \end{aligned} \quad (44)$$

or, upon expanding eq. (41),

$$\begin{aligned} & \sum_{l=0}^{\infty} \sum_{m=-l}^l \left[ \left( \frac{2+l(l+1)}{r^2} E_{lm}^{\perp} - \frac{2}{r} \frac{dE_{lm}^{\perp}}{dr} - \frac{d^2 E_{lm}^{\perp}}{dr^2} - \frac{2l(l+1)}{r^2} E_{lm}^{(1)} - k^2 \epsilon \right) \mathbf{Y}_{lm} \right. \\ & + \left( -\frac{2}{r^2} E_{lm}^{\perp} - \frac{2}{r} \frac{dE_{lm}^{(1)}}{dr} - \frac{d^2 E_{lm}^{(1)}}{dr^2} + \frac{l(l+1)}{r^2} E_{lm}^{(1)} - k^2 \epsilon \right) \mathbf{\Psi}_{lm} \\ & \left. + \left( -\frac{2}{r} \frac{dE_{lm}^{(2)}}{dr} - \frac{d^2 E_{lm}^{(2)}}{dr^2} + \frac{l(l+1)}{r^2} E_{lm}^{(2)} - k^2 \epsilon \right) \mathbf{\Phi}_{lm} \right] = i \frac{4\pi k}{c} \mathbf{j} - \frac{4\pi}{\epsilon} \nabla \rho. \end{aligned} \quad (45)$$

For notional simplicity we did not write the vector harmonics expansion on the RHS (inhomogeneous term) of both equations, which is straightforward, however. Taking into

account the closure relations of the vector spherical harmonics both equations reduce to a system of three ordinary differential equations for each vector spherical harmonics. Note furthermore that only the first two are coupled, respectively, whereas the last one can be solved independently. We proceed by first solving the coupled system of the first two. Subtracting the  $\Psi_{lm}$  expansion coefficients of both equations gives

$$\frac{1}{r} \frac{dE_{lm}^\perp}{dr} + \frac{2}{r^2} E_{lm}^\perp - \frac{l(l+1)}{r^2} E_{lm}^{(1)} = \frac{4\pi}{\epsilon} (\nabla \rho)_{lm}^{(1)} \quad (46)$$

or

$$E_{lm}^{(1)} = \frac{r}{l(l+1)} \frac{dE_{lm}^\perp}{dr} + \frac{2}{l(l+1)} E_{lm}^\perp - \frac{4\pi}{\epsilon l(l+1)} r^2 (\nabla \rho)_{lm}^{(1)}. \quad (47)$$

Inserting into the  $\mathbf{Y}_{lm}$  expansion coefficient of eq. (44) then leads to

$$\frac{l(l+1)}{r^2} E_{lm}^\perp - \frac{l(l+1)}{r} \frac{dE_{lm}^\perp}{dr} - \frac{1}{r} \frac{dE_{lm}^\perp}{dr} - \frac{2}{r^2} E_{lm}^\perp - k^2 \epsilon E_{lm}^\perp = i \frac{4\pi k}{c} j_{lm}^\perp - \frac{4\pi}{\epsilon} (\nabla \rho)_{lm}^{(1)}. \quad (48)$$

We finally compute the derivative of the  $E_{lm}^{(1)}$  term by inserting eq. (47)

$$\begin{aligned} & - \frac{1}{r} \frac{d}{dr} \left( \frac{r dE_{lm}^\perp}{dr} + 2E_{lm}^\perp - \frac{4\pi}{\epsilon} r^2 (\nabla \rho)_{lm}^{(1)} \right) - \frac{1}{r} \frac{dE_{lm}^\perp}{dr} + \left( \frac{l(l+1)-2}{r^2} - k^2 \epsilon \right) E_{lm}^\perp \\ & = i \frac{4\pi k}{c} j_{lm}^\perp - \frac{4\pi}{\epsilon} (\nabla \rho)_{lm}^{(1)} \end{aligned} \quad (49)$$

obtaining

$$r^2 \frac{d^2 E_{lm}^\perp}{dr^2} + 4r \frac{dE_{lm}^\perp}{dr} + (k^2 \epsilon r^2 - l(l+1) + 2) E_{lm}^\perp = -i \frac{4\pi k}{c} j_{lm}^\perp + \frac{12\pi}{\epsilon} (\nabla \rho)_{lm}^{(1)} + \frac{4\pi}{\epsilon} r \frac{d(\nabla \rho)_{lm}^{(1)}}{dr} \quad (50)$$

or (after setting  $E_{lm}^\perp = E_{lm}^{(\perp)}/r$ )

$$r^2 \frac{d^2 E_{lm}^{(\perp)}}{dr^2} + 2r \frac{dE_{lm}^{(\perp)}}{dr} + (k^2 \epsilon r^2 - l(l+1)) E_{lm}^{(\perp)} = -i \frac{4\pi k}{c} r j_{lm}^\perp + \frac{12\pi}{\epsilon} r (\nabla \rho)_{lm}^{(1)} + \frac{4\pi}{\epsilon} r^2 \frac{d(\nabla \rho)_{lm}^{(1)}}{dr}. \quad (51)$$

This is an inhomogeneous second order differential equation in  $E_{lm}^{(\perp)}$  of (modified) spherical Bessel equation type (after absorbing  $k\sqrt{|\epsilon|} = kn$  into  $r$ ). The fate of the equation being of modified type or not is decided by the sign of the index of refraction  $n = \sqrt{\epsilon}$ . While in vacuum  $n$  is positive corresponding to a spherical Bessel equation, within the sphere both positive and negative sign (depending on the frequency considered can occur). In the following, we consider the negative sign leading to evanescent excitations (i.e., modified Bessel functions in the interior) confined to the surface of the sphere, which corresponds to localized surface plasmons. The third equation has the same structure

$$r^2 \frac{d^2 E_{lm}^{(2)}}{dr^2} + 2r \frac{dE_{lm}^{(2)}}{dr} + (r^2 k^2 n^2 - l(l+1)) E_{lm}^{(2)} = -i \frac{4\pi k}{c} j_{lm}^{(2)}. \quad (52)$$

Both sets of solutions are independent. Note furthermore that the solution space can be further restricted by only admitting solutions, which do not diverge at the origin (i.e. modified

spherical Bessel functions of the first kind in the interior). The homogeneous solution to the first expansion then explicitly reads

$$E_{lm}^{(\perp)}(r) = \begin{cases} a_l^{(\perp)} i_l(nkr) & r < R \\ b_l^{(\perp)} j_l(kr) + c_l^{(\perp)} y_l(kr) & r \geq R, \end{cases} \quad (53)$$

and from eq. (47)

$$E_{lm}^{(1)}(r) = \begin{cases} a_l^{(\perp)} \left[ \frac{nk}{l(l+1)} i_{l+1}(nkr) + \frac{1}{l} \frac{i_l(nkr)}{r} \right] & r < R \\ b_l^{(\perp)} \left( \frac{k}{l(l+1)} j_{l-1}(kr) + \frac{1}{(l+1)} \frac{j_l(kr)}{r} \right) + c_l^{(\perp)} \left( \frac{k}{l(l+1)} y_{l-1}(kr) + \frac{1}{(l+1)} \frac{y_l(kr)}{r} \right) & r \geq R. \end{cases} \quad (54)$$

The second solution reads

$$E_{lm}^{(2)}(r) = \begin{cases} a_l^{(2)} i_l(nkr) & r < R \\ b_l^{(2)} j_l(kr) + c_l^{(2)} y_l(kr) & r \geq R. \end{cases} \quad (55)$$

In the first case the magnetic field is strictly tangential to the sphere, whereas in the second case the electric field is tangential. In accordance with the convention employed for the plane boundary (i.e. sphere radius  $\rightarrow \infty$ ) they are called transverse magnetic (TM) and transverse electric (TE) modes. Note furthermore that in both cases the homogeneous solutions are degenerate with respect to  $m$ .

## B.2 Boundary Conditions

In order to determine the 6 expansion coefficients of the homogeneous solutions above we require 4 BCs (two for  $E^{(\perp)}$  and two for  $E^{(2)}$ ) for each homogeneous domain,  $E^{(1)}$  can be computed once  $E^{(\perp)}$  is known. The two remaining degrees of freedom are fixed by normalization of the TM and TE modes respectively. We begin with the internal boundaries at the surface of the sphere. Indeed, it is only at this stage, where deviations from the classical Mie theory are introduced by the axion term as we anticipated. These boundary conditions are derived from partial derivatives normal to the surface as usual:

1. Boundary condition from the second Maxwell equation

$$E_{lm1}^{(1)} = E_{lm2}^{(1)} \quad (56)$$

and hence

$$\frac{rdE_{lm1}^{\perp}}{dr} + 2E_{lm1}^{\perp} = \frac{rdE_{lm2}^{\perp}}{dr} + 2E_{lm2}^{\perp}. \quad (57)$$

2. Boundary condition from the third Maxwell equation

$$\hat{r} \cdot \mathbf{B}_2 - \hat{r} \cdot \mathbf{B}_1 = 0 \quad (58)$$

$$-\frac{l(l+1)}{r} (E_{lm1}^{(2)} - E_{lm2}^{(2)}) = 0. \quad (59)$$



3. Boundary condition from the first Maxwell equation ( $\hat{\mathbf{r}} \hat{=} \text{outward unit normal}$ )

$$\hat{\mathbf{r}} \mathbf{D}_2 - \hat{\mathbf{r}} \mathbf{D}_1 = \frac{i\alpha\Theta_2}{k\pi} \hat{\mathbf{r}} \cdot (\nabla \times \mathbf{E}_2) - \frac{i\alpha\Theta_1}{k\pi} \hat{\mathbf{r}} \cdot (\nabla \times \mathbf{E}_1) \quad (60)$$

reads

$$\begin{aligned} n_2^2 E_{lm2}^\perp - n_1^2 E_{lm1}^\perp &= \frac{i\alpha\Theta_2}{k\pi} \hat{\mathbf{r}} \cdot (\nabla \times \mathbf{E}_2) - \frac{i\alpha\Theta_1}{k\pi} \hat{\mathbf{r}} \cdot (\nabla \times \mathbf{E}_1) \\ E_{lm2}^\perp - n^2 E_{lm1}^\perp &= -\frac{i\alpha\Theta_2}{k\pi} \frac{l(l+1)}{r} E_{lm2}^{(2)} + \frac{i\alpha\Theta_1}{k\pi} \frac{l(l+1)}{r} E_{lm1}^{(2)} \\ &= \frac{i\alpha}{k\pi} \frac{l(l+1)}{r} E_{lm}^{(2)} \Theta \end{aligned} \quad (61)$$

where the last line is obtained after inserting the continuity of the  $E_{lm}^{(2)}$  components derived from the second boundary condition eq. (59) and using  $\Theta_2 = 0$  (topological trivial material outside of the sphere) and  $\Theta_1 = \Theta$ .

4. Boundary condition from the fourth Maxwell equation ( $\hat{\mathbf{t}}^{1,2} \hat{=} \text{tangent unit vector into } \Psi_{lm} \text{ and } \Phi_{lm} \text{ direction}$ )

$$\frac{\alpha}{\pi} (\hat{\mathbf{t}}^1 \mathbf{E}_1 \Theta_1 - \hat{\mathbf{t}}^1 \mathbf{E}_2 \Theta_2) = (\hat{\mathbf{t}}^1 \mathbf{B}_1 - \hat{\mathbf{t}}^1 \mathbf{B}_2) \quad (62)$$

and hence

$$\frac{\alpha}{\pi} (E_{lm1}^{(1)} \Theta_1 - E_{lm2}^{(1)} \Theta_2) = -\frac{1}{ik} \left[ \left( \frac{dE_{lm1}^{(2)}}{dr} + \frac{1}{r} E_{lm1}^{(2)} \right) - \left( \frac{dE_{lm2}^{(2)}}{dr} + \frac{1}{r} E_{lm2}^{(2)} \right) \right] \quad (63)$$

Upon inserting eq. (47) we obtain

$$\begin{aligned} &\frac{\alpha r^2}{\pi l(l+1)} \left( \left( \frac{dE_{lm1}^\perp}{r dr} + \frac{2}{r^2} E_{lm1}^\perp \right) \Theta_1 - \left( \frac{dE_{lm2}^\perp}{r dr} + \frac{2}{r^2} E_{lm2}^\perp \right) \Theta_2 \right) \\ &= -\frac{1}{ik} \left[ \left( \frac{dE_{lm1}^{(2)}}{dr} + \frac{1}{r} E_{lm1}^{(2)} \right) - \left( \frac{dE_{lm2}^{(2)}}{dr} + \frac{1}{r} E_{lm2}^{(2)} \right) \right] \end{aligned} \quad (64)$$

and finally

$$\begin{aligned} &\frac{\alpha}{\pi l(l+1)} \left( \left( r \frac{dE_{lm1}^\perp}{dr} + 2E_{lm1}^\perp \right) \Theta_1 - \left( r \frac{dE_{lm2}^\perp}{dr} + 2E_{lm2}^\perp \right) \Theta_2 \right) \\ &= -\frac{1}{ik} \left[ \left( \frac{dE_{lm1}^{(2)}}{dr} \right) - \left( \frac{dE_{lm2}^{(2)}}{dr} \right) \right] \end{aligned} \quad (65)$$

or using BC1 eq. (57)

$$\frac{\alpha}{\pi l(l+1)} \left( r \frac{dE_{lm}^\perp}{dr} + 2E_{lm}^\perp \right) \Theta = -\frac{1}{ik} \left[ \left( \frac{dE_{lm1}^{(2)}}{dr} \right) - \left( \frac{dE_{lm2}^{(2)}}{dr} \right) \right] \quad (66)$$

completing the 4 required BCs. Similarly to the field equations only 2 of the 4 BCs are affected by the topological term (i.e., those pertaining to the inhomogeneous Maxwell equations), while the other two remain as in the classical Mie theory.

We finally solve the system of BCs for the 6 coefficients  $a_l$ ,  $b_l$ ,  $c_l$ ; the two free degrees of freedom (we only have 4 BCs) are fixed by the normalization of the TM and TE modes respectively as noted previously.

$$\left( \begin{array}{cccccc|c} a_l^{(\perp)} & b_l^{(\perp)} & c_l^{(\perp)} & a_l^{(2)} & b_l^{(2)} & c_l^{(2)} & \\ \hline \frac{di_l}{dr} + \frac{i_l}{r} & -\frac{dj_l}{dr} - \frac{j_l}{r} & -\frac{dy_l}{dr} - \frac{y_l}{r} & 0 & 0 & 0 & 0 \\ 0 & 0 & 0 & i_l & -j_l & -y_l & 0 \\ -n^2 i_l & j_l & y_l & -\frac{i\alpha l(l+1)\Theta}{k\pi} i_l & 0 & 0 & 0 \\ \frac{ik\alpha\Theta}{\pi l(l+1)} \left( \frac{di_l}{dr} + \frac{i_l}{r} \right) & 0 & 0 & \frac{di_l}{dr} & -\frac{dj_l}{dr} & -\frac{dy_l}{dr} & 0 \end{array} \right) \quad (67)$$

Solutions of the equation system for  $b_l^{(2)}$ ,  $c_l^{(2)}$ ,  $b_l^{(\perp)}$  and  $c_l^{(\perp)}$  in terms of  $a_l^{(\perp)}$  and  $a_l^{(2)}$ :

$$b_l^{(2)} = \frac{a_l^{(2)} \left( y_l \frac{di_l}{dr} - i_l \frac{dy_l}{dr} \right)}{y_l \frac{dj_l}{dr} - j_l \frac{dy_l}{dr}} + \frac{a_l^{(\perp)} \frac{ik\alpha\Theta}{\pi l(l+1)} \frac{d(ri_l)}{rdr} y_l}{y_l \frac{dj_l}{dr} - j_l \frac{dy_l}{dr}} \quad (68)$$

$$c_l^{(2)} = \frac{a_l^{(2)} \left( j_l \frac{di_l}{dr} - i_l \frac{dj_l}{dr} \right)}{j_l \frac{dy_l}{dr} - y_l \frac{dj_l}{dr}} + \frac{a_l^{(\perp)} \frac{ik\alpha\Theta}{\pi l(l+1)} \frac{d(ri_l)}{rdr} j_l}{j_l \frac{dy_l}{dr} - y_l \frac{dj_l}{dr}} \quad (69)$$

$$b_l^{(\perp)} = \frac{a_l^{(\perp)} \left( y_l \frac{d(ri_l)}{rdr} - n^2 i_l \frac{d(ry_l)}{rdr} \right)}{y_l \frac{dj_l}{dr} - j_l \frac{dy_l}{dr}} + \frac{a_l^{(2)} \frac{\alpha l(l+1)\Theta}{ik\pi} \frac{d(ry_l)}{rdr} i_l}{y_l \frac{dj_l}{dr} - j_l \frac{dy_l}{dr}} \quad (70)$$

$$c_l^{(\perp)} = \frac{a_l^{(\perp)} \left( j_l \frac{d(ri_l)}{rdr} - n^2 i_l \frac{d(rj_l)}{rdr} \right)}{j_l \frac{dy_l}{dr} - y_l \frac{dj_l}{dr}} + \frac{a_l^{(2)} \frac{\alpha l(l+1)\Theta}{ik\pi} \frac{d(rj_l)}{rdr} i_l}{j_l \frac{dy_l}{dr} - y_l \frac{dj_l}{dr}} \quad (71)$$

In order to obtain an analytic expression of the scattering and extinction cross section ( $\sigma_s$  eq. (75) and  $\sigma_e$  eq. (74)) one first re-expresses the normal modes in the vacuum regions in terms of Hankel functions of first and second kind with excitation coefficients

$$d_l = \frac{b_l - ic_l}{2} \quad \text{and} \quad e_l = \frac{b_l + ic_l}{2} \quad (72)$$

which allow a separation of incoming and outgoing spherical waves. In a second step the outgoing waves are normalized with the incoming one to obtain the normalized scattered wave and the scattering cross section. Finally the coefficients  $a_l^{(\perp)}$  or  $a_l^{(2)}$  are fixed by requiring the outgoing waves  $d_l^{(\perp)}$  or  $d_l^{(2)}$  to be zero respectively. In explicit form we obtain for the TM mode

$$f_l^{(\perp)} = \frac{d_l^{(\perp)} - e_l^{(\perp)}}{-2e_l^{(\perp)}} = \frac{n^2 i_l \frac{d(rj_l)}{rdr} - j_l \frac{d(ri_l)}{rdr} + \alpha^2 \Theta^2 \zeta \frac{d(rj_l)}{rdr}}{n^2 i_l \frac{d(rh_l^{(1)})}{rdr} - h_l^{(1)} \frac{d(ri_l)}{rdr} + \alpha^2 \Theta^2 \zeta \frac{d(rh_l^{(1)})}{rdr}} \quad (73)$$

$$\text{with } \zeta = \frac{\frac{d(ri_l)}{rdr} h_l^{(2)}}{\pi^2 \left( \frac{di_l}{dr} h_l^{(2)} - i_l \frac{dh_l^{(2)}}{dr} \right)} i_l$$

and for the TE mode

$$g_l^{(2)} = \frac{d_l^{(2)} - e_l^{(2)}}{-2e_l^{(2)}} = \frac{i_l \frac{d(rj_l)}{rdr} - j_l \frac{dri_l}{rdr} + \alpha^2 \Theta^2 \xi j_l}{i_l \frac{drh_l^{(1)}}{rdr} - h_l^{(1)} \frac{dri_l}{rdr} + \alpha^2 \Theta^2 \xi h_l^{(1)}} \quad (74)$$

$$\text{with } \xi = \frac{i_l \frac{d(rh_l^{(2)})}{rdr}}{\pi^2 \left( \frac{d(ri_l)}{rdr} h_l^{(2)} - n^2 i_l \frac{d(rh_l^{(2)})}{rdr} \right)} \frac{d(ri_l)}{rdr}$$

respectively.

Note that we get an additional factor of  $-\frac{1}{2}$  in the definition of  $f_l^{(\perp)}$  and  $g_l^{(2)}$  in comparison to the well-known classical Mie theory result (see, e.g., [20]). This is a consequence of our choice of the vector spherical harmonics defined by Barrera et al. [23]. The scattering cross section  $\sigma_s$  and extinction cross section  $\sigma_e$  then reads:

$$\begin{aligned} \sigma_s &= \frac{2\pi}{k^2} \sum_{l=0}^{\infty} (2l+1) \left( |f_l^{(\perp)}|^2 + |g_l^{(2)}|^2 \right) \\ &= \frac{2\pi}{k^2} \sum_{l=0}^{\infty} (2l+1) \\ &\times \left( \left| \frac{n^2 i_l \frac{d(rj_l)}{rdr} - j_l \frac{d(ri_l)}{rdr} + \alpha^2 \Theta^2 \zeta \frac{d(rj_l)}{rdr}}{n^2 i_l \frac{d(rh_l^{(1)})}{rdr} - h_l^{(1)} \frac{d(ri_l)}{rdr} + \alpha^2 \Theta^2 \zeta \frac{d(rh_l^{(1)})}{rdr}} \right|^2 + \left| \frac{i_l \frac{d(rj_l)}{rdr} - j_l \frac{dri_l}{rdr} + \alpha^2 \Theta^2 \xi j_l}{i_l \frac{drh_l^{(1)}}{rdr} - h_l^{(1)} \frac{dri_l}{rdr} + \alpha^2 \Theta^2 \xi h_l^{(1)}} \right|^2 \right) \end{aligned} \quad (75)$$

and

$$\begin{aligned} \sigma_e &= \frac{2\pi}{k^2} \sum_{l=0}^{\infty} (2l+1) \Re \left\{ f_l^{(\perp)} + g_l^{(2)} \right\} \\ &= \frac{2\pi}{k^2} \sum_{l=0}^{\infty} (2l+1) \\ &\times \Re \left\{ \frac{n^2 i_l \frac{d(rj_l)}{rdr} - j_l \frac{d(ri_l)}{rdr} + \alpha^2 \Theta^2 \zeta \frac{d(rj_l)}{rdr}}{n^2 i_l \frac{d(rh_l^{(1)})}{rdr} - h_l^{(1)} \frac{d(ri_l)}{rdr} + \alpha^2 \Theta^2 \zeta \frac{d(rh_l^{(1)})}{rdr}} + \frac{i_l \frac{d(rj_l)}{rdr} - j_l \frac{dri_l}{rdr} + \alpha^2 \Theta^2 \xi j_l}{i_l \frac{drh_l^{(1)}}{rdr} - h_l^{(1)} \frac{dri_l}{rdr} + \alpha^2 \Theta^2 \xi h_l^{(1)}} \right\} \end{aligned} \quad (74)$$

These are the classical Mie theory results for the TM and TE mode (typically derived by employing Hertz potentials, see, e.g., [20]) modified by the axion term.

## References

- [1] E. Witten, *Dyons of charge  $e/2$* , Physics Letters B **86**(3), 283 (1979), doi:[https://doi.org/10.1016/0370-2693\(79\)90838-4](https://doi.org/10.1016/0370-2693(79)90838-4).
- [2] K. Fujikawa and H. Suzuki, *Path integrals and quantum anomalies*, 122. Oxford University Press on Demand (2004).
- [3] H. Nielsen and M. Ninomiya, *The Adler-Bell-Jackiw anomaly and Weyl fermions in a crystal*, Physics Letters B **130**(6), 389 (1983), doi:[https://doi.org/10.1016/0370-2693\(83\)91529-0](https://doi.org/10.1016/0370-2693(83)91529-0).

- [4] F. Wilczek, *Two applications of axion electrodynamics*, Phys. Rev. Lett. **58**, 1799 (1987), doi:10.1103/PhysRevLett.58.1799.
- [5] E. Fradkin, E. Dagotto and D. Boyanovsky, *Physical Realization of the Parity Anomaly in Condensed Matter Physics*, Phys. Rev. Lett. **57**, 2967 (1986), doi:10.1103/PhysRevLett.57.2967.
- [6] M. Z. Hasan and C. L. Kane, *Colloquium: Topological insulators*, Rev. Mod. Phys. **82**, 3045 (2010), doi:10.1103/RevModPhys.82.3045.
- [7] X.-L. Qi and S.-C. Zhang, *Topological insulators and superconductors*, Rev. Mod. Phys. **83**, 1057 (2011), doi:10.1103/RevModPhys.83.1057.
- [8] B. Yan and C. Felser, *Topological Materials: Weyl Semimetals*, Annual Review of Condensed Matter Physics **8**, 337 (2017), doi:10.1146/annurev-conmatphys-031016-025458.
- [9] X.-L. Qi, T. L. Hughes and S.-C. Zhang, *Topological field theory of time-reversal invariant insulators*, Phys. Rev. B **78**, 195424 (2008), doi:10.1103/PhysRevB.78.195424.
- [10] X.-L. Qi, R. Li, J. Zang and S.-C. Zhang, *Inducing a Magnetic Monopole with Topological Surface States*, Science **323**(5918), 1184 (2009), doi:10.1126/science.1167747.
- [11] A. Karch, *Electric-Magnetic Duality and Topological Insulators*, Phys. Rev. Lett. **103**, 171601 (2009), doi:10.1103/PhysRevLett.103.171601.
- [12] A. Karch, *Surface plasmons and topological insulators*, Phys. Rev. B **83**, 245432 (2011), doi:10.1103/PhysRevB.83.245432.
- [13] S. Ryu, J. E. Moore and A. W. W. Ludwig, *Electromagnetic and gravitational responses and anomalies in topological insulators and superconductors*, Phys. Rev. B **85**, 045104 (2012), doi:10.1103/PhysRevB.85.045104.
- [14] A. Martín-Ruiz, M. Cambiaso and L. F. Urrutia, *Electromagnetic description of three-dimensional time-reversal invariant ponderable topological insulators*, Phys. Rev. D **94**, 085019 (2016), doi:10.1103/PhysRevD.94.085019.
- [15] F. S. Nogueira, Z. Nussinov and J. van den Brink, *Fractional Angular Momentum at Topological Insulator Interfaces*, Phys. Rev. Lett. **121**, 227001 (2018), doi:10.1103/PhysRevLett.121.227001.
- [16] F. S. Nogueira and J. van den Brink, *Absence of magnetic monopoles in Maxwellian magnetoelectrics*, <https://arxiv.org/abs/1808.08825> (2018), arXiv:1808.08825.
- [17] L. Wu, M. Salehi, N. Koirala, J. Moon, S. Oh and N. P. Armitage, *Quantized Faraday and Kerr rotation and axion electrodynamics of a 3D topological insulator*, Science **354**(6316), 1124 (2016), doi:10.1126/science.aaf5541.
- [18] V. Dziom, A. Shuvaev, A. Pimenov, G. V. Astakhov, C. Ames, K. Bendias, J. Böttcher, G. Tkachov, E. M. Hankiewicz, C. Brüne, H. Buhmann and L. W. Molenkamp, *Observation of the universal magnetoelectric effect in a 3D topological insulator*, Nature Communications **8**, 15197 (2017), doi:10.1038/ncomms15197;.

- [19] G. Mie, *Beiträge zur Optik trüber Medien, speziell kolloidaler Metallösungen*, Annalen der Physik **330**(3), 377 (1908), doi:10.1002/andp.19083300302.
- [20] C. Bohren and D. Huffman, *Absorption and Scattering of Light by Small Particles*, Wiley, ISBN 9780471293408 (1983).
- [21] W. T. Grandy Jr and W. T. Grandy, *Scattering of waves from large spheres*, Cambridge University Press (2005).
- [22] L. Ge, D. Han and J. Zi, *Electromagnetic scattering by spheres of topological insulators*, Optics Communications **354**, 225 (2015), doi:https://doi.org/10.1016/j.optcom.2015.05.054.
- [23] R. G. Barrera, G. A. Estevez and J. Giraldo, *Vector spherical harmonics and their application to magnetostatics*, European Journal of Physics **6**(4), 287 (1985), doi:10.1088/0143-0807/6/4/014.
- [24] J. Krehl, G. Guzzinati, J. Schultz, P. Potapov, D. Pohl, J. Martin, J. Verbeeck, A. Fery, B. Büchner and A. Lubk, *Spectral field mapping in plasmonic nanostructures with nanometer resolution*, Nature Communications **9**(1), 4207 (2018), doi:10.1038/s41467-018-06572-9.